Ecological Modelling xxx (2018) xxx–xxx

Contents lists available at ScienceDirect

Ecological Modelling

journal homepage: www.elsevier.com/locate/ecolmodel

Exploitative competition of invaders differentially influences the diversity of neutral, lumpy and intransitive phytoplankton assemblages in spatially heterogeneous environments

Joydeb Bhattacharyya[a], Daniel L. Roelke[a,b,*], Rika M.W. Muhl[a], Frances G. Withrow[a]

[a] Department of Wildlife and Fisheries Sciences, Texas A&M University, 2258 TAMUS, College Station, TX 77843-2258, USA
[b] Department of Oceanography, Texas A&M University, College Station, TX 77843, USA

ARTICLE INFO

Article history:
Received 18 July 2017
Received in revised form
22 December 2017
Accepted 30 December 2017
Available online xxx

Keywords:
Biodiversity
Species supersaturation
Spatial heterogeneity
Circulation
Invasion

ABSTRACT

Recent theoretical research suggested that species-supersaturated phytoplankton assemblages sustained through neutrality, lumpy coexistence or intransitivity were sensitive to immigration, quickly losing diversity following invasions. The presence of source patches, however, may facilitate persistence of species-supersaturation in the face of invaders. We explore that notion here through simulation analyses of more detailed spatially explicit models depicting one- and two-dimensional systems ("pipe" and "two-eddy" models, respectively) where water circulation is governed over a range of advection and turbulent diffusion. For the pipe model, when advection and turbulent diffusion are low, and when advection is high and turbulent diffusion is low, resident assemblages are more resistant to invaders. But at intermediate rates of advection and with increases to turbulent diffusion, assemblages are more quickly impacted by invaders. For the two-eddy model, when advection and turbulent diffusion are low, resident assemblages are again resistant to invaders, but only for lumpy assemblages. In contrast to the "pipe" model, resistance to invaders of neutral and lumpy assemblages is high when advection and turbulent diffusion are high. For both model configurations, intransitive assemblages were much more sensitive to invaders, suggesting that intransitivity might not be as prevalent a biodiversity-sustaining mechanism in spatially heterogeneous plankton systems.

1. Introduction

In theory, exclusion through exploitative resource competition will lead to a number of co-existing species not greater than the number of limiting resources as systems approach equilibrium. High species richness characteristic of many biological systems challenges this idea, coined the "Paradox of the Plankton" (Hutchinson, 1961). One solution to this paradox occurs due to fluctuations in the environment, thereby preventing equilibrium conditions (Tilman, 1977, 1981, 1982; Sommer, 1984, 1985; Grover, 1989). Environmental fluctuations can arise through various abiotic and biotic processes that change seasonally, contributing to periodic cycling of plankton populations (Smayda, 1985; Nixon, 1995; Roelke and Spatharis, 2015). The effects of these fluctuations can also result in protracted periods of transient population dynamics (Hastings, 2010) or chaotic population dynamics (May and Leonard, 1975). Both of these dynamic types can facilitate species richness. However, there are other mechanisms that are not externally-driven that lead to high species richness (Narwani et al., 2009). For example, competition for nutrients can create internal disequilibria that can sustain high species richness in phytoplankton assemblages (Huisman and Weissing, 1994). In addition, neutrality, lumpy coexistence and intransitive population dynamics, the focus of this research, are biodiversity-sustaining mechanisms which occur in assemblages based on competitive abilities of co-occurring species.

Neutrality refers to the co-occurrence of species within a given trophic level that are nearly identical in their competitive abilities and can be considered ecological equivalents (Hubbell, 2001). With neutrality, multiple species can coexist over ecologically relevant time scales, promoting higher biodiversity. Neutrality was shown for biological systems of wasps (Saez and Lozano, 2005), fungi (Bickford et al., 2007), and trees (McGill, 2003), and might also

* Corresponding author at: Department of Wildlife and Fisheries Sciences, Texas A&M University, 2258 TAMUS, College Station, TX 77843-2258, USA.
E-mail address: droelke@tamu.edu (D.L. Roelke).

https://doi.org/10.1016/j.ecolmodel.2017.12.020
0304-3800/

be a mechanism underlying high species richness in phytoplankton assemblages (Chust et al., 2013; Roelke and Eldridge, 2008).

Where there are co-occurring and competing species clusters along resource gradients, the condition is referred to as lumpy coexistence (Scheffer and van Nes, 2006). With lumpy coexistence, species with very similar competitive abilities co-occur within a cluster. The clusters, however, are sufficiently different from each other so that competition occurs between them. Example communities showing lumpy coexistence include wetland plants in Mediterranean-type ecosystems (Valiente-Banuet et al., 2006), aquatic beetles (Drost et al., 1992) and prairie birds (Holling, 1992). In theory, lumpy coexistence can explain highly diverse phytoplankton systems as well (Scheffer and van Nes, 2006; Roelke and Eldridge, 2008).

When competition for resources between co-existing species is non-hierarchical, intransitive population dynamics can result. With intransitive assemblages, no single species can displace all other species and recurrent, out-of-phase oscillations in population dynamics occur (Huisman et al., 1999; Huisman and Weissing, 2001a,b; Roelke and Eldridge, 2010). Biological systems involving coral reef invertebrates (Jackson and Buss, 1975), side-blotched lizards (Sinervo and Lively, 1996), and herbaceous dicots (Fortner and Weltzin, 2007) are examples of naturally occurring intransitive systems. In theory, intransitivity supports high richness in phytoplankton assemblages as well (Huisman and Weissing, 2001a,b).

In a previous modeling study, Roelke and Eldridge (2008) explored the effect of migration on phytoplankton assemblages whose biodiversity was sustained either by neutrality, lumpy coexistence or intransitivity. They explored a plankton model where the influence of migration was a function of hydraulic mixing. Using a two-patch modeling framework, they found that immigration, even at very low levels, led to global homogenization and species extinctions. From these observations, they questioned the role of neutrality, lumpy coexistence and intransitivity as biodiversity-sustaining mechanisms in natural environments. The two-patch modeling framework used in Roelke and Eldridge (2008), however, might have been too simple to allow for source-sink patches to develop, which are known to facilitate biodiversity (Mouquet and Loreau, 2003).

In this research, we develop two models of greater spatial complexity, thus enabling source-sink patch development. The models employ one-dimensional and two-dimensional horizontal frameworks with various hydrology. The distribution of organisms in our models are subject to advection and turbulent diffusion. In advection, the nutrients and the embedded phytoplankton cells are carried with the movement of water. In turbulent diffusion, the spatial mixing of nutrients and phytoplankton of adjacent patches occurs without a net overall transport of water. Advection and turbulent diffusion were shown to be important to phytoplankton richness and diversity (Codeco and Grover, 2001; Petrovskii and Malchow, 2001; McKiver et al., 2009; Adjou et al., 2012). Here, we explored these over spatial scales >100 km with 10 km^2 areal resolution and at turbulent diffusion rates characteristic of large lakes, bays and coastal oceans. We employ one- and two-dimensional model frameworks. Our one-dimensional model framework is best visualized as two pipes coming together at an outlet where flow through the pipes are advection- and turbulent diffusion-based (Fig. 1). Our two-dimensional model framework is best visualized as two confined eddies that are in contact, rotating in opposite directions, and again with advective and turbulent diffusive flow (Fig. 2). Through simulation analyses, we explore and compare the resistance of phytoplankton assemblage source patches initiated with neutral, lumpy and intransitive phytoplankton assemblages under varied hydraulic conditions.

2. Methods

2.1. One-dimensional model

In our one-dimensional model, $R_{i,k}(t)$ and $P_{j,k}(t)$ represent the concentration of the growth-limiting i-th substrate (μM) and the population density of j-th phytoplankton species ($\times 10^6$ cells L^{-1}), respectively, in the k-th patch at time t. The rate of flushing and the rate of mixing between two adjacent patches are taken as D and d (day^{-1}), respectively (these are discussed in detail further below). The specific growth rate for the j-th phytoplankton species in the k-th patch is determined using the Monod equation (Monod, 1949) and Liebig's law of the Minimum (Liebig, 1840), and is given by

$$\mu_{j,k} = \mu_{\max,j}\left(\min_i\left(\frac{R_{i,k}}{a_{i,j}+R_{i,k}}\right)\right),$$

where $\mu_{max,j}$ is the maximum specific growth rate (day^{-1}) of species j and $a_{i,j}$ is the half- saturation coefficient (μM) of species j growing on the substrate i. Here, we use the notation "a" instead of the traditional notation "k_S" for convenience with subscript appending. Finally, $Q_{i,j}$ is the fixed cellular content of resource i (μM (10^6 cells)$^{-1}$) for species j.

For our one-dimensional physical framework, we define the system as having an odd number ($2n+1$) of interconnecting patches, out of which the direction of advection in the first and the last patches are pointed towards each other (Fig. 1). In addition, the $(n+1)^{th}$ patch, which receives advection originating from the first and last patches, has an advection rate twice the rate of advection of all the other patches. Also, there is a constant inflow to the first and last patches, bringing new nutrients R_i^{in} to the system. Finally, the first and last patch only contain the initial phytoplankton assemblages (described further below). As the simulation proceeds, these source assemblages disperse by means of advection and turbulent diffusion.

The one-dimensional model is governed by sets of discretized ordinary differential equations necessary for representing both end member patches (1^{st} and $(2n+1)^{th}$), the central patch ($(n+1)^{th}$), and patches in between (2^{nd}–n^{th}, $(n+2)^{th}$–$2n^{th}$). The rate of change of the nutrients in each of the patches is dependent on the advection-driven nutrient input and flushing rate, turbulent diffusion-driven nutrient mixing rate with adjacent patches and nutrient consumption rate by phytoplankton. The rate of change of the phytoplankton density in each of the patches is dependent on the growth rate of phytoplankton, advection-driven hydraulic displacement of phytoplankton and turbulent diffusion-driven exchange rate of phytoplankton.

The governing equations for resources and phytoplankton for the first patch are given by:

$$\frac{dR_{i,1}}{dt} = D(R_i^{in} - R_{i,1}) + d(R_{i,2} - R_{i,1}) - \Sigma_j Q_{i,j}\mu_{j,1}P_{j,1} \quad (1)$$

$$\frac{dP_{j,1}}{dt} = \mu_{j,1}P_{j,1} + d(P_{j,2} - P_{j,1}) - DP_{j,1} \quad (2)$$

The governing equations for resources and phytoplankton for the last patch ($(2n+1)^{th}$) are given by:

$$\frac{dR_{i,2n+1}}{dt} = D(R_i^{in} - R_{i,2n+1}) + d(R_{i,2n} - R_{i,2n+1}) - \Sigma_j Q_{i,j}\mu_{j,2n+1}P_{j,2n+1} \quad (3)$$

$$\frac{dP_{j,2n+1}}{dt} = \mu_{j,2n+1}P_{j,2n+1} + d(P_{j,2n} - P_{j,2n+1}) - DP_{j,2n+1} \quad (4)$$

For each of the patches in between the first and middle patch, designated with $k = 2, \ldots, n$, resources and phytoplankton are governed by:

$$\frac{dR_{i,k}}{dt} = D(R_{i,k-1} - R_{i,k}) + d(R_{i,k-1} + R_{i,k+1}) - 2dR_{i,k} - \Sigma_j Q_{i,j}\mu_{j,k}P_{j,k} \quad (5)$$

Please cite this article in press as: Bhattacharyya, J., et al., Exploitative competition of invaders differentially influences the diversity of neutral, lumpy and intransitive phytoplankton assemblages in spatially heterogeneous environments. Ecol. Model. (2018), https://doi.org/10.1016/j.ecolmodel.2017.12.020

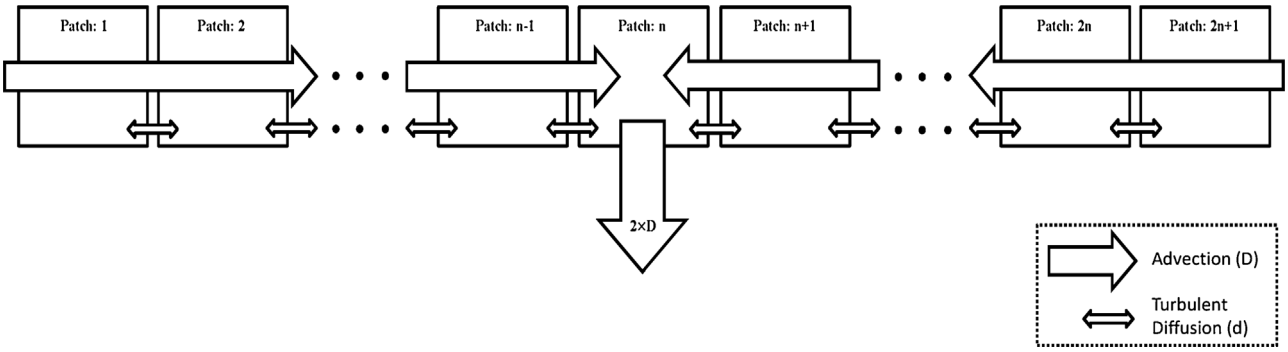

Fig. 1. One-dimensional model framework, where advective flows (thicker block arrows) carrying source nutrients enter the model domain from either end of the model "pipe" configuration. Advective flows carrying ambient nutrients and phytoplankton cells exits the model domain from the middle of the "pipe" configuration. Patches of the model "pipe" configuration also exchange ambient nutrients and phytoplankton cells through turbulent diffusion (thinner block arrows). Initial phytoplankton assemblages were at either end of the "pipe" configuration, i.e., patches 1 and 2n + 1.

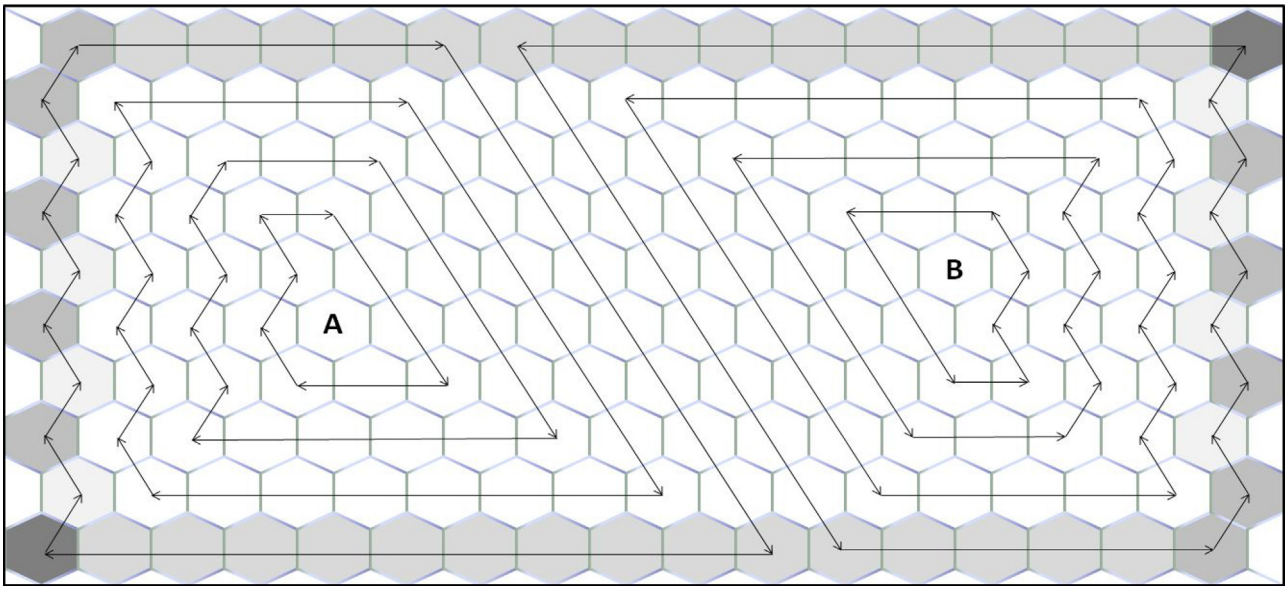

Fig. 2. Two-dimensional model framework, where advective flows (arrows) carrying ambient nutrients and phytoplankton cells form adjacent eddies rotating in opposite directions. Turbulent diffusion occurs between all touching hexagonal patches. Because the model domain is closed, interior patches (white) are most influenced by eddy diffusion and patches on edges (lighter greys) and corners (dark grey) of the model domain are progressively less influenced by eddy diffusion. Initial phytoplankton assemblages were in the center of the eddies, i.e., patches A and B.

$$\frac{dP_{j,k}}{dt} = \mu_{j,k}P_{j,k} + D(P_{j,k-1} - P_{j,k}) + d(P_{j,k-1} + P_{j,k+1}) - 2dP_{j,k} \quad (6)$$

For each of the patches in between the middle and last patch, designated with $k = n+2, \ldots, 2n$, resources and phytoplankton are governed by:

$$\frac{dR_{i,k}}{dt} = D(R_{i,k+1} - R_{i,k}) + d(R_{i,k+1} + R_{i,k-1}) - 2dR_{i,k} - \Sigma_j Q_{i,j}\mu_{j,k}P_{j,k} \quad (7)$$

$$\frac{dP_{j,k}}{dt} = \mu_{j,k}P_{j,k} + D(P_{j,k+1} - P_{j,k}) + d(P_{j,k+1} + P_{j,k-1}) - 2dP_{j,k} \quad (8)$$

And for the middle patch, $n+1$, the governing equations for resources and phytoplankton are:

$$\frac{dR_{i,n+1}}{dt} = (D+d)(R_{i,n} - 2R_{i,n+1} + R_{i,n+2}) - \Sigma_j Q_{i,j}\mu_{j,n+1}P_{j,n+1} \quad (9)$$

$$\frac{dP_{j,n+1}}{dt} = \mu_{j,n+1}P_{j,n+1} + (D+d)(P_{j,n} - 2P_{j,n+1} + P_{j,n+2}), \quad (10)$$

where $R_{i,k}(0) \geq 0$ and $P_{j,k}(0) \geq 0$.

2.2. Two-dimensional framework

For our two-dimensional model framework, we define the model domain as two eddies in contact, one rotating clockwise and the other rotating counter clockwise (Fig. 2). The patches of this modeling framework are of hexagonal geometry. In this two-dimensional model framework there are $2n$ number of circulation rings about each of the eddy cores (patches A and B). The indexing of the circulation rings start from the closest ring to the core of the eddy. There are a total $2(2n+1)(8n+1)$ patches in our two-dimensional model framework, represented by a grid with $2(2n+1)$ rows and $8n+1$ columns. Each of the patches has a constant upward diffusion of nutrients R_i^{in} by means of an assumed uniform vertical mixing at a rate V day^{-1}. The sinking of phytoplankton species in each of the patches is also uniform at the rate V day^{-1}. Finally, the patches A and B have the initial phytoplankton assemblages which spread to the adjacent patches by means of advection and turbulent diffusion.

In our two-dimensional model, $R_{i,k,l}(t)$ and $P_{j,k,l}(t)$ represent the concentration of the growth-limiting i-th resource (μM) and the population density of j-th phytoplankton species ($\times 10^6$ cells

Please cite this article in press as: Bhattacharyya, J., et al., Exploitative competition of invaders differentially influences the diversity of neutral, lumpy and intransitive phytoplankton assemblages in spatially heterogeneous environments. Ecol. Model. (2018), https://doi.org/10.1016/j.ecolmodel.2017.12.020

L^{-1}), respectively, in the patch (k, l) at time t. As with the one-dimensional "pipe" model, here the rate of change of the nutrients in each of the patches is dependent on advection-driven nutrient input and flushing rate, turbulent diffusion-driven nutrient mixing rate with adjacent patches and nutrient consumption rate by phytoplankton. Similar to before, the rate of change of phytoplankton in each of the patches is dependent on the growth rate of phytoplankton, advection-driven immigration and hydraulic displacement of phytoplankton, and turbulent diffusion-driven exchange of phytoplankton. In each of the interior patches surrounding the source patch A, the mixing of substrates and phytoplankton by means of turbulent diffusion are given by $R^I_{i,k,l}$ and $P^I_{j,k,l}$ respectively, where

$R^I_{i,k,l} = R_{i,k,l-1} + R_{i,k,l+1} + R_{i,k-1,l-1+\delta} + R_{i,k-1,l+\delta} + R_{i,k+1,l-1+\delta} + R_{i,k+1,l+\delta} - 6R_{i,k,l}$, $P^I_{j,k,l} = P_{j,k,l-1} + P_{j,k,l+1} + P_{j,k-1,l-1+\delta} + P_{j,k-1,l+\delta} + P_{j,k+1,l-1+\delta} + P_{j,k+1,l+\delta} - 6P_{j,k,l}$, and $\delta = 0$ or 1 accordingly when k is even or odd.

The governing equations for resources and phytoplankton in the source patches (A and B, see Fig. 2) are given by:

$$\frac{dR_{i,k,l}}{dt} = (R_i^{in} - R_{i,k,l})V + dR^I_{i,k,l} - \Sigma_j Q_{i,j}\mu_{j,k,l}P_{j,k,l} \quad (11)$$

$$\frac{dP_{j,k,l}}{dt} = \mu_{j,k,l}P_{j,k,l} + dP^I_{j,k,l} - VP_{j,k,l}, \quad (12)$$

where (k, l) is either ($2n+2$, $2n+1$) or ($2n+1$, $6n+1$) according to whether the source patch is at A or B respectively, and

$$\mu_{j,k,l} = \mu_{\max,j}\left(\min_i\left(\frac{R_{i,k,l}}{a_{i,j} + R_{i,k,l}}\right)\right).$$

Each interior patch, associated with the $2n-1$ circulations around the source A is governed by one of the following four sets of differential equations

$$\frac{dR_{i,k,l}}{dt} = (R_i^{in} - R_{i,k,l})V + D(R_{i,k+1,l-1+\delta} - R_{i,k,l}) + dR^I_{i,k,l} - \Sigma_j Q_{i,j}\mu_{j,k,l}P_{j,k,l} \quad (13)$$

$$\frac{dP_{j,k,l}}{dt} = \mu_{j,k,l}P_{j,k,l} + D(P_{j,k+1,l-1+\delta} - P_{j,k,l}) + dP^I_{j,k,l} - VP_{j,k,l}, \quad (14)$$

$$\frac{dR_{i,k,l}}{dt} = (R_i^{in} - R_{i,k,l})V + D(R_{i,k-1,l-1+\delta} - R_{i,k,l}) + dR^I_{i,k,l} - \Sigma_j Q_{i,j}\mu_{j,k,l}P_{j,k,l} \quad (15)$$

$$\frac{dP_{j,k,l}}{dt} = \mu_{j,k,l}P_{j,k,l} + D(P_{j,k-1,l-1+\delta} - P_{j,k,l}) + dP^I_{j,k,l} - VP_{j,k,l}, \quad (16)$$

$$\frac{dR_{i,k,l}}{dt} = (R_i^{in} - R_{i,k,l})V + D(R_{i,k,l-1} - R_{i,k,l}) + dR^I_{i,k,l} - \Sigma_j Q_{i,j}\mu_{j,k,l}P_{j,k,l} \quad (17)$$

$$\frac{dP_{j,k,l}}{dt} = \mu_{j,k,l}P_{j,k,l} + D(P_{j,k,l-1} - P_{j,k,l}) + dP^I_{j,k,l} - VP_{j,k,l}, \quad (18)$$

$$\frac{dR_{i,k,l}}{dt} = (R_i^{in} - R_{i,k,l})V + D(R_{i,k,l+1} - R_{i,k,l}) + dR^I_{i,k,l} - \Sigma_j Q_{i,j}\mu_{j,k,l}P_{j,k,l} \quad (19)$$

$$\frac{dP_{j,k,l}}{dt} = \mu_{j,k,l}P_{j,k,l} + D(P_{j,k,l+1} - P_{j,k,l}) + dP^I_{j,k,l} - VP_{j,k,l}, \quad (20)$$

More specifically, (13) and (14) govern the patches along left edges including the top-left patch, (15) and (16) govern the patches along top edges including the top-right patch, (17) and (18) govern the patches along right edges including the bottom-right patch, and (19) and (20) govern the patches along bottom edges including the bottom-left patch (see Fig. 2).

The upper and lower boundary patches of the outermost circulation (excluding the corner patches) about the source patch A are governed by the differential equations

$$\frac{dR_{i,k,l}}{dt} = (R_i^{in} - R_{i,k,l})V + D(R_{i,k,l-1} - R_{ikl}) + dR^{TB}_{i,k,l} - \Sigma_j Q_{i,j}\mu_{j,k,l}P_{j,k,l} \quad (21)$$

$$\frac{dP_{j,k,l}}{dt} = \mu_{j,k,l}P_{j,k,l} + DP^{TB}_{i,k,l} - VP_{j,k,l}, \quad (22)$$

where $R^{TB}_{i,k,l} = R_{i,k,l-1} + R_{i,k,l+1} + R_{i,k+p,l-2+\rho} + R_{i,k+p,l-1+\rho} - 4R_{i,k,l}$ and $P^{TB}_{j,k,l} = P_{i,k,l-1} + P_{i,k,l+1} + P_{i,k+p,l-2+\rho} + P_{i,k+p,l-1+\rho} - 4P_{i,k,l}$, $p = (-1)^\rho$, $\rho = 1$ or 2 according to whether the boundary patch is at the bottom or at the top of the circulation.

The left boundary patches of the outermost circulation (excluding the corner patches) about A are governed by

$$\frac{dR_{i,k,l}}{dt} = (R_i^{in} - R_{i,k,l})V + D(R_{i,k,l+1} - R_{i,k,l}) + dR^L_{i,k,l} - \Sigma_j Q_{i,j}\mu_{j,k,l}P_{j,k,l} \quad (23)$$

$$\frac{dP_{j,k,l}}{dt} = \mu_{j,k,l}P_{j,k,l} + D(P_{i,k,l+1} - P_{i,k,l}) + dP^L_{i,k,l} - VP_{j,k,l}, \quad (24)$$

where $R^L_{i,k,l} = R_{i,k,l+1} + R_{i,k-1,l} + \delta R_{i,k-1,l+1} + R_{i,k+1,l} + \delta R_{i,k+1,l+1} - (3+2\delta)R_{i,k,l}$ and $P^L_{j,k,l} = P_{i,k,l+1} + P_{i,k-1,l} + \delta P_{i,k-1,l+1} + P_{i,k+1,l} + \delta P_{i,k+1,l+1} - (3+2\delta)P_{i,k,l}$.

The right boundary patches (excluding the corner patches) about A are governed by

$$\frac{dR_{i,k,l}}{dt} = (R_i^{in} - R_{i,k,l})V + D(R_{i,k-1,l-1+\delta} - R_{i,k,l}) + dR^I_{i,k,l} - \Sigma_j Q_{i,j}\mu_{j,k,l}P_{j,k,l} \quad (25)$$

$$\frac{dP_{j,k,l}}{dt} = \mu_{j,k,l}P_{j,k,l} + D(P_{j,k-1,l-1+\delta} - P_{j,k,l}) + dP^I_{j,k,l} - VP_{j,k,l}, \quad (26)$$

The bottom left, top left, top right and bottom right corner patches are governed by

$$\frac{dR_{i,k,l}}{dt} = (R_i^{in} - R_{i,k,l})V + D(R_{i,k,l+1} - R_{i,k,l}) + dR^{BL}_{i,k,l+1} - \Sigma_j Q_{i,j}\mu_{j,k,l}P_{j,k,l} \quad (27)$$

$$\frac{dP_{j,k,l}}{dt} = \mu_{j,k,l}P_{j,k,l} + D(P_{i,k,l+1} - P_{i,k,l}) + dP^{BL}_{i,k,l+1} - VP_{j,k,l}, \quad (28)$$

$$\frac{dR_{i,k,l}}{dt} = (R_i^{in} - R_{i,k,l})V + D(R_{i,k+1,l} - R_{i,k,l}) + dR^{TL}_{i,k,l+1} - \Sigma_j Q_{i,j}\mu_{j,k,l}P_{j,k,l} \quad (29)$$

$$\frac{dP_{j,k,l}}{dt} = \mu_{j,k,l}P_{j,k,l} + D(P_{i,k+1,l} - P_{i,k,l}) + dP^{TL}_{i,k,l+1} - VP_{j,k,l}, \quad (30)$$

$$\frac{dR_{i,k,l}}{dt} = (R_i^{in} - R_{i,k,l})V + D(R_{i,k,l-1} - R_{i,k,l}) + dR^{TR}_{i,k,l+1} - \Sigma_j Q_{i,j}\mu_{j,k,l}P_{j,k,l} \quad (31)$$

$$\frac{dP_{j,k,l}}{dt} = \mu_{j,k,l}P_{j,k,l} + D(P_{i,k,l-1} - P_{i,k,l}) + dP^{TR}_{i,k,l+1} - VP_{j,k,l}, \quad (32)$$

$$\frac{dR_{i,k,l}}{dt} = (R_i^{in} - R_{i,k,l})V + D(R_{i,k-1,l-1} - R_{i,k,l}) + dR^{BR}_{i,k,l+1} - \Sigma_j Q_{i,j}\mu_{j,k,l}P_{j,k,l} \quad (33)$$

$$\frac{dP_{j,k,l}}{dt} = \mu_{j,k,l}P_{j,k,l} + D(P_{i,k-1,l-1} - P_{i,k,l}) + dP^{BR}_{i,k,l+1} - VP_{j,k,l}, \quad (34)$$

respectively, where

$$R^{BL}_{i,k,l+1} = R_{i,k,l+1} + R_{i,k-1,l} - 2R_{i,k,l},$$

$$R^{TL}_{i,k,l+1} = R_{i,k,l+1} + R_{i,k+1,l} + R_{i,k+1,l+1} - 3R_{i,k,l},$$

$$R^{TR}_{i,k,l+1} = R_{i,k,l-1} + R_{i,k,l+1} + R_{i,k+1,l} + R_{i,k+1,l+1} - 4R_{i,k,l},$$

$$R^{BR}_{i,k,l+1} = R_{i,k,l-1} + R_{i,k,l+1} + R_{i,k-1,l-1} + R_{i,k-1,l} - 4R_{i,k,l},$$

$$P^{BL}_{i,k,l+1} = P_{i,k,l+1} + P_{i,k-1,l} - 2P_{i,k,l},$$

$$P^{TL}_{i,k,l+1} = P_{i,k,l+1} + P_{i,k+1,l} + P_{i,k+1,l+1} - 3P_{i,k,l},$$

$$P^{TR}_{i,k,l+1} = P_{i,k,l-1} + P_{i,k,l+1} + P_{i,k+1,l} + P_{i,k+1,l+1} - 4P_{i,k,l}, \quad \text{and}$$

$$P^{BR}_{i,k,l+1} = P_{i,k,l-1} + P_{i,k,l+1} + P_{i,k-1,l-1} + P_{i,k-1,l} - 4P_{i,k,l}.$$

The patches corresponding to the circulation about the source B are governed by the differential equations similar to Eqs. (13)–(34) with a counter clockwise advection flow pattern.

Please cite this article in press as: Bhattacharyya, J., et al., Exploitative competition of invaders differentially influences the diversity of neutral, lumpy and intransitive phytoplankton assemblages in spatially heterogeneous environments. Ecol. Model. (2018), https://doi.org/10.1016/j.ecolmodel.2017.12.020

2.3. Initial conditions, parameterizations, hydrology, and numeric technique

Population densities of species comprising phytoplankton assemblages in the initial condition was 0.1×10^6 cells liter^{-1} in patches 1 and $(2n+1)$ for the one-dimensional model and patches *A* and *B* for the two dimensional model. All other patches in both models had zero phytoplankton initially. Initial resource concentrations in all patches was 10 μM. For this research, we have considered speciose assemblages, each of neutral, lumpy and intransitive assemblage types (Roelke and Eldridge, 2008). For the one- and two-dimensional frameworks, simulations are based on all possible combinations of assemblages, chosen two at a time, from a similar assemblage biodiversity type (i.e., either neutral, lumpy or intransitive). There are 10 assemblages per assemblage biodiversity type, thus there are 45 assemblage combinations for each (135 total assemblage combinations when considering all three assemblage diversity types). The maximum specific growth rate ($\mu_{max,j}$) of each phytoplankton species is taken as 1 (day^{-1}). The values of $a_{i,j}$ and $Q_{i,j}$ were provided in Roelke and Eldridge (2008). For this research we have considered three resources, where assigned values to parameters associated with the first resource (*R*, *a* and *Q*) are based on nitrogen and assigned values to parameters associated with the other two resources are considered as nitrogen-equivalents.

For our simulation analyses, we examined how source patch diversity is influenced by different rates of advection and turbulent diffusion. The range of advection used in our simulations is from 0 to 1 day^{-1}, not exceeding the maximum specific growth rate of phytoplankton species. When considering 10 km^2 patches with 3.162 km distances between central locations, this range in advection rate is 0–0.1318 km h^{-1}. The rates of turbulent diffusion explored here range from 0.05 to 0.3 d^{-1}, which equates to 5.787×10^4 cm^2 s^{-1} to 3.472×10^5 cm^2 s^{-1} when considering 10 km^2 areas of patches in the "pipe" configuration of the model and 5.012×10^4 cm^2 s^{-1} to 3.007×10^5 cm^2 s^{-1} when considering 8.660 km^2 areas of patches in the "two-eddy" configuration of the model (still with 3.162 km distances between central locations). These rates of turbulent diffusion are typical in large lakes, bays and coastal oceans (Okubo, 1971; Peeters and Hofmann, 2015; Matsuzaki and Fujita, 2017). Peclet number (*Pe*), a dimensionless measure of advection to turbulent diffusion over a target distance, was as low as 0 in our simulations where there was no advection, and as high as ~20 for the "pipe" configuration at our highest advection rate and lowest turbulent diffusion rate, and as high as ~23 for the "two-eddy" configuration at our highest advection rate and lowest turbulent diffusion rate. This range in *Pe* spans hydraulic conditions where delivery of nutrients to phytoplankton via fluid motion becomes increasingly important relative to diffusive flux alone, i.e., Pe > 1 (Reynolds, 2006). For the one-dimensional framework, we have considered 11 interconnecting patches ($n = 5$), whereas for the two-dimensional treatment, a total 170 patches are considered ($n = 2$) in 10 rows and 17 columns with four circulation rings about the eddy cores.

We employed numerical techniques to solve the mathematical equations of our one- and two-dimensional models using MATLAB-ODE-solving routines based on fourth-order Runge-Kutta procedures with a variable time step based on a local error tolerance of 10^{-6}.

2.4. Response variable

We examine the change in diversity with time in each of the source patches as estimated according to Shannon's diversity index (Shannon and Weaver, 1949). For the one dimensional model framework, the Shannon diversity index in source patch at day *t* is given by:

$$H(t) = -\sum_j p_j(t)\, LN p_j(t)$$

where p_j is the proportion the species *j* to the total phytoplankton.

To objectively quantify the amount of time until a resident phytoplankton assemblage became compromised by invaders, we used the rate of change in diversity of the source patch. We decided this approach after qualitatively observing diversity collapses in various simulations, whose onset could be seen just after source patch diversity peaked. To quantify, we use a five-point formula to determine the derivative of the diversity curve ($H_k(t)$) from the source patch. The set $\Omega_{k,\ t_0} = \{t \in R_+ : f_k(t) f_k(t+1) < 0,\ t \geq t_0\}$ represented the days after the initial t_0 days when there are changes in curvature of $H_k(t)$, where $f_k(t) = \frac{-H_k(t+2)+8H_k(t+1)-8H_k(t-1)+H_k(t-2)}{12}$. The change in curvature of the diversity curve just after the initial t_0 days is given by $t_k = \inf \Omega_{k,t_0}$, where t_k exists if and only if $\Omega_{k,t_0} \neq \phi$. If $\Omega_{k,\ t_0} = \phi$, then the value of t_k is set equal to the upper time limit of the model simulations. If $P^R_{j,k}$ and $P^I_{j,k}$ represent the resident and invader species respectively in the source patch *k*, where $P_{j,k} = P^R_{j,k} + P^I_{j,k}$, then the total invader biomass at the t_kth day is given by $P^I_k = \Sigma_j P^I_{j,k}$. For all 45 different combinations of neutral assemblages, we obtain a set of t_k (in days) together with a set of total invader biomass $(P^I_k)_{Neutral}$ ($\times 10^6$ cells liter^{-1}). The average of these values gives the number of days taken by the neutral assemblages after the initial t_0 days of simulation to lose its integrity, and the corresponding average invader biomass. For the 45 lumpy assemblage combinations, we use the same procedure to find the average number of days after the initial t_0 days when there is a change in orientation of the diversity curve and the corresponding average invader biomass. The average invader biomass in neutral and lumpy assemblages is given by $P^I_{k,avg} = \frac{1}{2}\left(\frac{(P^I_k)_{Neutral}+(P^I_k)_{Lumpy}}{^{10}C_2}\right)$. Since the 45 intransitive assemblage combinations have oscillatory dynamics, we use $P^I_{k,avg}$ as the threshold to find the average number of days taken by the total invader biomass of intransitive assemblages to cross the threshold value. For the two dimensional model framework, we use the same approach to find the average number of days taken by the three types of assemblages to start losing their identity due to the invaders.

3. Results

Resident phytoplankton assemblages in the source patches became compromised by invaders, regardless of assemblage type. But the assemblage types differed in how long that period was before becoming compromised. In general, neutral and lumpy assemblages in source patches took the longest amount of time to become compromised (representative simulations are shown in Fig. 3a and b). The population dynamics were similar as well, with smooth changes that asymptotically approached maxima or minima, or changes that peaked before declining (Fig. 3d and e). In contrast, intransitive assemblages in source patches took the shortest amount of time (representative simulation shown in Fig. 3c) with erratic population dynamics quickly approaching towards maxima or minima, or towards a maximum before declining (Fig. 3f).

For the "pipe" configuration of the model, the period of time until assemblages became compromised by invaders varied as a function of hydrology, but differentially between the assemblage types. For example, neutral assemblages showed greater resistance to invaders when advection and turbulent diffusion were low, and when advection was high and turbulent diffusion low, both

Please cite this article in press as: Bhattacharyya, J., et al., Exploitative competition of invaders differentially influences the diversity of neutral, lumpy and intransitive phytoplankton assemblages in spatially heterogeneous environments. Ecol. Model. (2018), https://doi.org/10.1016/j.ecolmodel.2017.12.020

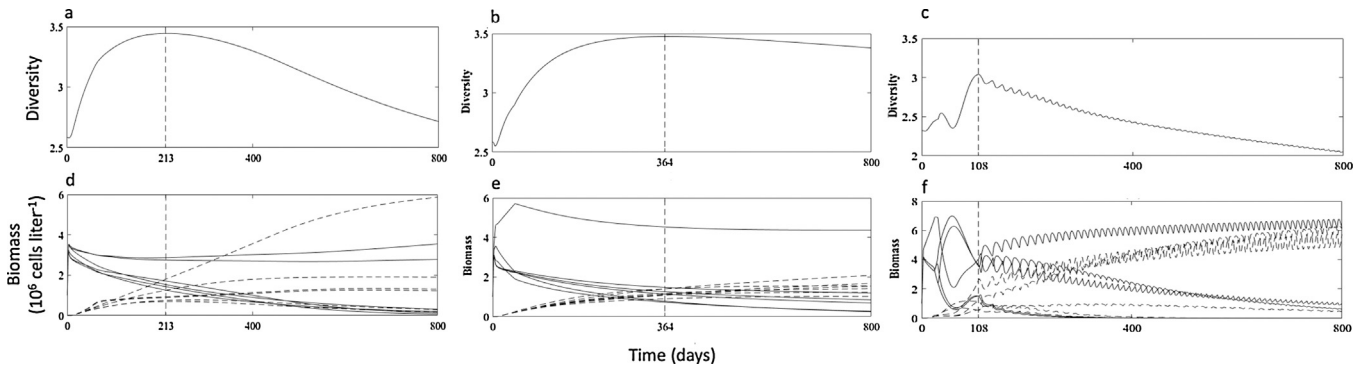

Fig. 3. Representative diversity and population dynamics for neutral (a and d), lumpy (b and e), and intransitive (c and f) assemblages. Solid and dashed lines in panels d, e and f indicate resident and invader species, respectively. The timing of diversity maxima observed in panels a, b and c was used to define the period before resident assemblages became compromised by invading populations, which can be seen in panels d, e and f (vertical dotted lines).

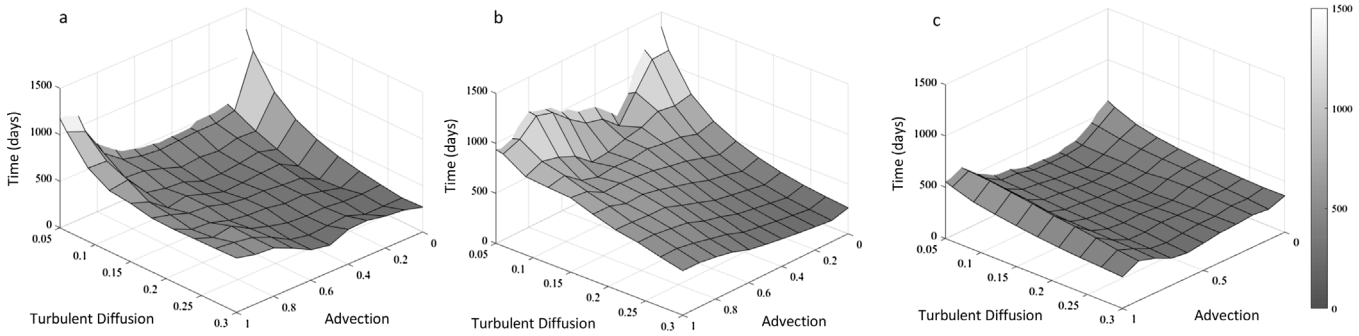

Fig. 4. The average (45 simulations per grid point) period of time until assemblages became compromised by invaders in the "pipe" configuration of the model. All combinations of advection and diffusion are shown for (a) neutral, (b) lumpy and (c) intransitive assemblages. In this configuration of the model, the distance between patch centers was 3.162 km, with area of each patch being 10 km^2. So, the advection maxima shown in the above panels of 1 d^{-1} was equivalent to 0.1318 km h^{-1}, and the range 0.05–0.3 d^{-1} for turbulent diffusion equates to a range of 5.787×10^4 cm^2 s^{-1}–3.472×10^5 cm^2 s^{-1}.

>1000 days (Fig. 4a). Otherwise, the period of time until assemblages became compromised was ~500 days. Lumpy assemblages in general showed greater resistance to invaders when turbulent diffusion was low, regardless of advection, with the period of time until assemblages became compromised ranging between ~1000 to ~1400 days (Fig. 4b). As turbulent diffusion increased, lumpy assemblages became compromised more quickly, taking ~250 days when advection was low and ~500 days when advection was high. Intransitive assemblages showed a trend similar to neutral assemblages, but less pronounced with maxima and minima until assemblages became compromised by invaders with times of ~600 and ~400 days, respectively (Fig. 4c). Regardless of assemblage type, nutrient concentrations in source patches were at their maxima (i.e., 10 μM) when advection was highest and turbulent diffusion lowest, which is the value of nutrient concentrations in the sources, and asymptotically decreased to minima (~0.1 μM) when advection was low (not shown).

For the "two-eddy" configuration of the model, the period of time until assemblages became compromised by invaders again varied as a function of hydrology, and again differentially between the assemblage types. For this model configuration, neutral assemblages showed greater resistance to invaders when advection and turbulent diffusion were higher, ~600 days (Fig. 5a). The period of time until neutral assemblages became compromised was least when turbulent diffusion was low, ranging between ~275 and ~300 days. Lumpy assemblages showed greater resistance to invaders when turbulent diffusion and advection were low, and when turbulent diffusion and advection were high, ~400 days (Fig. 5b). The period of time until lumpy assemblages became compromised was least when turbulent diffusion was low and advection high, ~225 days. As with the "pipe" configuration of the model, intransitive assemblages showed the greatest sensitivity to invaders in the "two-eddy" configuration. There was little difference in the times until assemblages became compromised, however, which was ~150 days at all combinations of advection and turbulent diffusion (Fig. 5c). Regardless of assemblage type, advection rate and turbulent diffusion rate, nutrient concentrations in source patches were depleted (~0.1 μM) (not shown).

4. Discussion

For the pipe configuration of the model, resident assemblages in the source patches are more resistant to invaders at the lowest and at higher advection rates, and when turbulent diffusion rates are low. Interestingly, at intermediate rates of advection, and while turbulent diffusion is low, resident assemblages are less resistant to invasions. This was true for all assemblage types. This trend at low turbulent diffusion rates occurs because as advection rate increases from a low value, greater hydraulic displacement of residents leads to lower biomass of resident populations. In turn, this leads to greater concentrations of nutrients, thereby lessening competitive advantages established residents might have had over invaders. This, then, facilitates invasions even as invaders originating from a downstream location must overcome a stronger current. But as advection rates further increase (from intermediate to higher values), invaders become less able to overcome currents. Even though nutrient concentrations in the source patch continue to increase with further decreases in biomass of residents, invaders are simply unable to arrive there in significant numbers and resistance of resident assemblages increases. So, there is an interplay between advection and turbulent diffusion rate in the pipe configuration of

Please cite this article in press as: Bhattacharyya, J., et al., Exploitative competition of invaders differentially influences the diversity of neutral, lumpy and intransitive phytoplankton assemblages in spatially heterogeneous environments. Ecol. Model. (2018), https://doi.org/10.1016/j.ecolmodel.2017.12.020

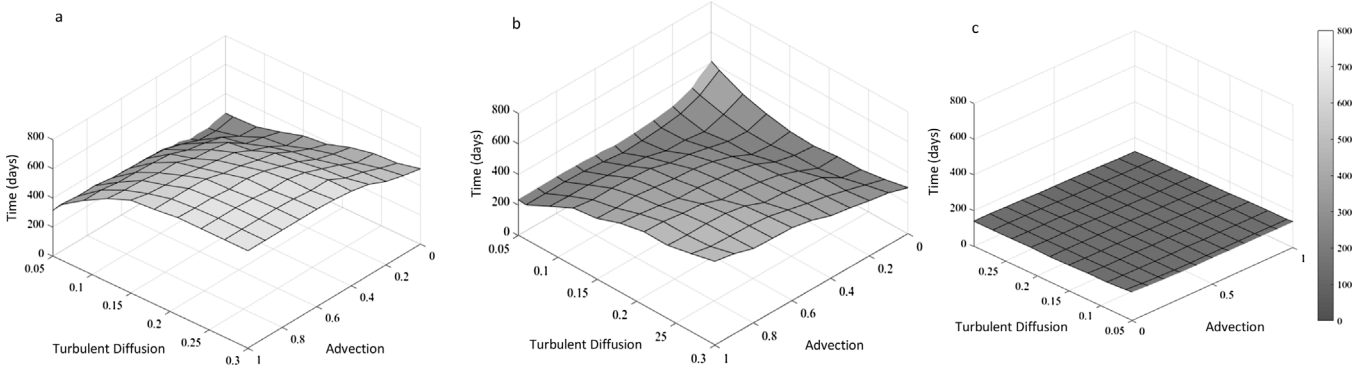

Fig. 5. The average (45 simulations per grid point) period of time until assemblages became compromised by invaders in the "two-eddy" configuration of the model. All combinations of advection and diffusion are shown for (a) neutral, (b) lumpy and (c) intransitive assemblages. In this configuration of the model, the distance between patch centers was 3.162 km, with area of each patch being 8.660 km^2. So, the advection maxima shown in the above panels of 1 d^{-1} was equivalent to 0.1318 km h^{-1}, and the range 0.05–0.3 d^{-1} for turbulent diffusion equates to a range of 5.012×10^4 cm^2 s^{-1}–3.007×10^5 cm^2 s^{-1}.

the model, where at low rates of turbulent diffusion an intermediate level of advection best facilitates invasion.

Our findings from the "pipe" configuration of the model are consistent, in part, with findings from others. For example, increased nutrient loadings with increased hydraulic displacements were shown to stimulate accumulation of downstream invader biomass in a model of similar configuration (Grover et al., 2017). Our findings showing poorer invasion success when advection is high and turbulent diffusion is low have also been observed in other models of similar configuration (Lutscher et al., 2005; Grover et al., 2011, 2017). In those models, increasing advection rates served as a mechanism preventing accumulation of downstream invader populations. Those models, however, depicted unidirectional advection throughout the model domain and employed hydraulic storage zones or source populations, neither of which are used here. The persistence of resident populations at higher advection rates in our model was due to sustained higher growth rates that occur with the higher nutrient loading rates, which has been described previously (Reynolds, 1990; Grover et al., 2009; Hsu et al., 2013). Our observation that assemblages become less resistant to downstream invaders as turbulent diffusion increases is also consistent with previous work (Grover et al., 2017).

For the two-eddy configuration of the model, when advection and turbulent diffusion rates are low, resident assemblages in source patches are again resistant to invaders, but only for lumpy assemblages. This is different from the pipe configuration of the model. Also in contrast to the pipe configuration model, resistance to invaders of neutral and lumpy assemblages is high when advection and turbulent diffusion rates are high. Factors leading to persistence of populations within circulating gyres, as depicted by our simulated eddies, show that circular advection and turbulent diffusion processes, in combination, lead to ageostrophic patterns that serve to retain populations within gyres when particles are positively buoyant (Zhong et al., 2012; Beron-Vera et al., 2015). Here, our particles are not positively buoyant, but our imposed sinking rate is not in excess of realized reproductive growth rates. The result is the same, in that resident populations are retained within eddies at higher rates of circular advection and turbulent diffusion, which leads to greater resistance to invaders, but again, only for neutral and lumpy phytoplankton assemblages.

Our findings show that resistance to invaders for neutral and lumpy assemblages are strongly dependent on the flow configurations. Intransitive assemblages in the pipe configuration of the model are also dependent on the flow configurations, but less so. In both configurations of the model, intransitive assemblages were more sensitive to invaders and unable to maintain source patches. The underpinning mechanism of high species diversity in intransitive phytoplankton assemblages, that is, intrinsic disturbances sustained by and promulgating species interactions (Huisman and Weissing, 1999, 2001a,b), were shown to require peculiar circumstances in regards to life history traits of co-occurring species and hydraulic conditions (Schippers et al., 2001; Roelke et al., 2003; Roelke and Eldridge, 2008, 2010). When those circumstances were violated, species diversity was lost. Those previous studies, however, were not of a configuration where source patches were depicted because they lacked adequate spatial domains. Here, we show that with a more complex spatial domain and over a wide range of hydrological conditions where source patches could be sustained, intransitive assemblages are still quite sensitive to invasions.

5. Conclusions

Our observations, along with those of Roelke and Eldridge (2008), suggest that intransitivity should not be a prevalent biodiversity-sustaining mechanism in spatially heterogeneous plankton systems, as it is much more sensitive to invaders than either neutrality or lumpy coexistence. On the other hand, neutral and lumpy coexistence mechanisms are more robust, suggesting a higher probability that they are biodiversity mechanisms in spatially heterogeneous plankton systems. In fact, in a recent modeling study (spatially homogeneous) it was shown that differences in nutrient supply fluctuation periodicities determined whether phytoplankton assemblages were comprised of near-neutral species or in species clusters along a temporally varying niche (Sakavara et al., 2017). In addition, a forthcoming analysis of plankton from eight lakes revealed persistence of species clusters in phytoplankton assemblages (Muhl et al., 2017).

We note, however, that even with our greater spatial complexity in this research effort, it may be that our modeling framework is still too simple to rule out intransitivity as a biodiversity sustaining mechanism in spatially heterogeneous phytoplankton systems. There are likely other processes influential that are not depicted here. For example, recently it was shown that interacting processes of light extinction, vertical mixing, particle sinking and benthic nutrient flux showed certain scenarios where the β-richness and β-diversity of intransitive assemblages are more resistant to environmental changes than for neutral or lumpy assemblages (Withrow et al., 2018). Similarly, in the Muhl et al. (2017) study mentioned above it was shown that intransitive assemblages are more resistant to allelopathic interactions than either neutral or lumpy assemblages, suggesting another condition by which intransitive assemblages might occur in spatially heterogeneous plankton environments.

Please cite this article in press as: Bhattacharyya, J., et al., Exploitative competition of invaders differentially influences the diversity of neutral, lumpy and intransitive phytoplankton assemblages in spatially heterogeneous environments. Ecol. Model. (2018), https://doi.org/10.1016/j.ecolmodel.2017.12.020

So, we can conclude from observations in the present study, combined with observations from these other studies, that when a system is primarily driven by two-dimensional hydrology and exploitative competition the incidence of supersaturated assemblages governed by intransitivity is less likely than the incidence of supersaturated assemblages governed by either neutrality or lumpy coexistence. This is not to say that speciose phytoplankton assemblages sustained by intransitivity do not occur in nature, as there are other environmental conditions and types of species interactions that may facilitate them.

References

Adjou, M., Bendtsen, J., Richardson, K., 2012. Modeling the influence from ocean transport, mixing and grazing on phytoplankton diversity. Ecol. Modell. 225, 19–27.
Beron-Vera, F.J., Olascoaga, J.M., Haller, G., Farazmand, M., Trinanes, J., Wang, Y., 2015. Dissipative inertial transport patterns near coherent Lagrangian eddies in the ocean. Chaos 25 (8), 087412.
Bickford, D., Lohman, D., Sodhi, N., Ng, P., Meier, R., Winker, K., Ingram, K., Das, I., 2007. Cryptic species as a window on diversity and conservation. Trends Ecol. Evol. 22, 148–155.
Chust, G., Irigoien, X., Chave, J., Harris, R.P., 2013. Latitudinal phytoplankton distribution and the neutral theory of biodiversity. Global Ecol. Biogeogr. 22, 531–543.
Codeco, C.T., Grover, J.P., 2001. Competition along a spatial gradient of resource supply: a microbial experimental model. Am. Nat. 157, 300–315.
Drost, M.B.H., Cuppen, H.P.J.S., Van Nieukerken, E.J., Schreijer, M., 1992. De Waterkevers van Nederland. Uitgeverij, Utrecht.
Fortner, A.M., Weltzin, J.F., 2007. Competitive hierarchy for four common old-field plant species depends on resource identity and availability. J. Torrey Bot. Soc. 134, 166–176.
Grover, J.P., Hsu, S.B., Wang, F.B., 2009. Competition and coexistence in flowing habitats with hydraulic storage zone. Math. Biosci. 222, 42–52.
Grover, J.P., Crane, K.W., Baker, J.W., Brooks, B.W., Roelke, D.L., 2011. Spatial variation of harmful algae and their toxins in flowing-water habitats: a theoretical exploration. J. Plankton Res. 33 (2), 211–227.
Grover, J.P., Roelke, D.L., Brooks, B.W., 2017. Population persistence in flowing-water habitats: conditions where flow-based management of harmful algal blooms works, and where it does not. Ecol. Eng. 99, 172–181.
Grover, J.P., 1989. Effects of Si:P supply ratio, supply variability, and selective grazing in the plankton: an experiment with a natural algal and protisan assemblage. Limnol. Oceanogr. 34 (2), 349–367.
Hastings, A., 2010. Timescales, dynamics, and ecological understanding. Ecol. Soc. Am. 91 (12), 3471–3480.
Holling, C.S., 1992. Cross-scale morphology, geometry, and dynamics of ecosystems. Ecol. Monogr. 62, 447–502.
Hsu, S.B., Wang, F.B., Zhao, X.Q., 2013. Global dynamics of zooplankton and harmful algae in flowing habitats. J. Differ. Equ. 255 (3), 265–297.
Hubbell, S.P., 2001. The Unified Neutral Theory of Biodiversity and Biogeography. Princeton University Press.
Huisman, J., Weissing, F.J., 1994. Light-limited growth and competition for light in well-mixed aquatic environments: an elementary model. Ecology 75, 507–520.
Huisman, J., Weissing, F.J., 2001a. Biological conditions for oscillations and chaos generated by multispecies competition. Ecology 82, 2682–2695.
Huisman, J., Weissing, F.J., 2001b. Fundamental unpredictability in multispecies competition. Am. Natur. 157, 488–494.
Huisman, J., Jonker, R., Zonneveld, C., Weissing, F., 1999. Competition for light between phytoplankton species: experimental tests of mechanistic theory. Ecology 80, 211–222.
Hutchinson, G.E., 1961. The paradox of the plankton. Am. Natur. 95, 137–145.
Jackson, J.B.C., Buss, L.W., 1975. Allelopathy and spatial competition among coral reef invertebrates. Proc. Natl. Acad. Sci. U. S. A. 72, 5160–5163.
Liebig, J., 1840. Die Chemie in ihrer Anvendung auf Agricultur, und Physiologic, 4th edition, 1847). Taylor and Walton, London.
Lutscher, F., Pachepsky, E., Lewis, M.A., 2005. The effect of dispersal patterns on stream populations. SIAM Rev. 47 (4), 749–772.
Matsuzaki, Y., Fujita, I., 2017. In situ estimates of horizontal turbulent diffusivity at the sea surface for oil transport simulation. Mar. Pollut. Bull. 117, 34–40.
May, R., Leonard, W., 1975. Nonlinear aspects of competition between three species. SIAM J. Appl. Math. 29, 243–253.
McGill, B., 2003. A test of the unified neutral theory of biodiversity. Lett. Nat. 422, 881–885.
McKiver, W., Neufeld, Z., Scheuring, I., 2009. Plankton bloom controlled by horizontal stirring. Nonlinear Processes Geophys. 16, 623–630.
Monod, J., 1949. The growth of bacterial cultures. Annu. Rev. Microbiol., 371–394.
Mouquet, N., Loreau, M., 2003. Community patterns in source-sink metacommunities. Am. Natur. 162, 544–557.
Muhl, R.M.W., Roelke, D.L., Bhattacharya, J., Withrow, F.G., 2017. Resisting annihilation: relationships between functional trait dissimilarity, self-organized biodiversity and allelopathy. In: 18th Workshop of the International Association of pPhytoplankton Taxonomy and Ecology (IAP), Natal, Rio Grande do Norte–Brazil, August 27–September 3, 2017.
Narwani, A., Berthin, J., Mazumder, A., 2009. Relative importance of endogenous and exogenous mechanisms in maintaining phytoplankton species diversity. Ecoscience 16, 429–440.
Nixon, S.W., 1995. Coastal marine eutrophication: a definition, social causes, and future concerns. Ophelia 41, 19–219.
Okubo, A., 1971. Ocean diffusion diagrams. Deep Sea Res. 18, 789–802.
Peeters, F., Hofmann, H., 2015. Length-scale dependence of horizontal dispersion in the surface water of lakes. Limnol. Oceanogr. 60, 1917–1934.
Petrovskii, S.V., Malchow, H., 2001. Wave of chaos: new mechanism of pattern formation in spatio-temporal population dynamics. Theor. Popul. Biol. 59, 157–174.
Reynolds, C.S., 1990. Temporal scales of variability in pelagic environments and the response of phytoplankton. Freshw. Biol. 23 (1), 25–53.
Reynolds, C.S., 2006. Ecology of Phytoplankton. Cambridge University Press, Cambridge, UK, 535 pages.
Roelke, D.L., Eldridge, P.M., 2008. Mixing of supersaturated assemblages and the precipitous loss of species. Am. Natur. 171, 162–175.
Roelke, D.L., Eldridge, P.M., 2010. Losers in the 'Rock-Paper-Scissors' game: the role of non-hierarchical competition and chaos as biodiversity sustaining agents in aquatic systems. Ecol. Model. 221, 1017–1027.
Roelke, D.L., Spatharis, S., 2015. Phytoplankton assemblage characteristics in recurrently fluctuating environments. PLoS One 10 (3), e0120673.
Roelke, D.L., Augustine, S., Buyukates, Y., 2003. Fundamental predictability in multispecies competition: the influence of large disturbance. Am. Natur. 162, 615–623.
Saez, A., Lozano, E., 2005. Body doubles. Nature 433, 111.
Sakavara, A., Tsirtsis, G., Roelke, D.L., Mancy, R., Spatharis, S., A new mechanism underpinning lumpy species coexistence in fluctuating resource environments. Proc. Natl. Acad. Sci. U. S. A., 2017 (early edition) doi/10.1073/pnas.1705944115.
Scheffer, M., van Nes, E.H., 2006. Self-organized similarity, the evolutionary emergence of groups of similar species. Proc. Natl. Acad. Sci. U. S. A. 103, 6230–6235.
Schippers, P., Verschoor, A.M., Vos, M., Mooij, W.M., 2001. Does supersaturated coexistence resolve the paradox of the plankton? Ecol. Lett. 4, 404–407.
Shannon, C.E., Weaver, W., 1949. The Mathematical Theory of Communication. Univ. Illinois Press, Urbana.
Sinervo, B., Lively, C.M., 1996. The rock-paper-scissors game and the evolution of alternative male strategies. Nature 380, 240–243.
Smayda, T.J., 1985. Narragansett Bay: variability and change in environment and phytoplankton dynamics over a 23-year period. Estuaries 8, 86.
Sommer, U., 1984. The paradox of the plankton: fluctuations of the phosphorus availability maintain diversity of phytoplankton in flow-through cultures. Limnol. Oceanogr. 29, 633–636.
Sommer, U., 1985. Comparison between steady state and non-steady state competition: experiments with natural phytoplankton. Limnol. Oceanogr. 30, 335–346.
Tilman, D., 1977. Resource competition between planktonic algae: an experimental and theoretical approach. Ecology 58, 338–348.
Tilman, D., 1981. Tests of resource competition theory using four species of Lake Michigan algae. Ecology 62, 802–815.
Tilman, D., 1982. Resource Competition and Community Structure. Princeton University Press, Princeton, NJ.
Valiente-Banuet, A., Rumebe, A.V., Miguel, V., 2006. Modern Quaternary plant lineages promote diversity through facilitation of ancient Tertiary lineages. Proc. Natl. Acad. Sci. U. S. A. 103, 16812–16817.
Withrow, F.G., Roelke, D.L., Muhl, R.M.W., Bhattacharyya, J., 2018. Water column processes differentially influence richness and diversity of neutral, lumpy and intransitive phytoplankton assemblages. Ecol. Model.
Zhong, Y., Bracco, A., Villareal, T.A., 2012. Pattern formation at the ocean surface: sargassum distribution and the role of the eddy field. Limnol. Oceanogr. Fluids Environ. 2 (1), 12–27.

Please cite this article in press as: Bhattacharyya, J., et al., Exploitative competition of invaders differentially influences the diversity of neutral, lumpy and intransitive phytoplankton assemblages in spatially heterogeneous environments. Ecol. Model. (2018), https://doi.org/10.1016/j.ecolmodel.2017.12.020